3rd URSI AT-AP-RASC, Gran Canaria, 29 May – 3 June 2022

Denoising Textile Kinematics Sensors: A Machine Learning Approach

Yuxuan Han, Vigyanshu Mishra, and Asimina Kiourti
ElectroScience Laboratory, Dept. of Electrical and Computer Engineering, The Ohio State University, USA

Abstract

Monitoring kinematics of the human body in real-world environments is beneficial to applications as diverse as healthcare, sports, human-machine interfaces, and more. To this end, we recently reported new classes of wearable textile-based sensors that consist of transmit/receive loops and operate based on Faraday's Law to seamlessly monitor joint flexion angles (e.g., knee, elbow, etc.). However, once embedded in fabrics, the loops will drift along with fabric movement and hence will impair the sensor's operation. In this work, we report a machine learning approach to model and remove noise associated with e-textile sensors being deformed upon the fabric (namely, e-textile noise), with a focus on kinematics monitoring applications.

1. Introduction

Today's "gold-standard" for monitoring kinematics entails the use of on-body retro-reflective markers tracked by infrared cameras [1]. Expectedly, this technique is limited to contrived environments. Alternative approaches have been reported, but they are again restricted to lab environments (markerless cameras); are obtrusive and suffer from integration drift (Inertial Measurement Units, IMUs); require line-of-sight (time-of-flight sensors); and/or obstruct natural movement (bending sensors) [1].

To overcome these limitations, we have recently reported new classes of e-textile sensors that can be embroidered into garments to monitor joint kinematics in the individual's natural environment [2-4]. By embroidering transmit (Tx) and receive (Rx) electrically small resonant loop antennas right above and below the joint (e.g., knee), respectively, the sensor can detect the relative angle between the two loops. However, a major challenge still persists: fabric deformation "in-the-wild" will deform the sensor and will add noise on the readings [5]. This noise will greatly compromise sensor performance, particularly during in-sport and on-field monitoring of kinematics (given the inherent fast-paced dynamic motion). As a result, a reliable method is needed to cancel the noise generated by fabric deformation, without compromising the sensor's seamlessness.

With the above in mind, we herewith model and remove noise associated with e-textile sensors being deformed upon the fabric (namely, e-textile noise), with a focus on kinematics monitoring applications. We remark that, to date, there are no studies of e-thread functionalized garments modeling the shift and/or deformation that occurs when a subject changes posture. Currently, unrealistic (fully symmetric) crumpling is assumed [6,7], or placement of the e-textile is suggested upon flat regions of the body (e.g., top of the shoulder) [8]. However, the latter is not feasible for e-textile kinematics sensors where loops may be placed anywhere on the body. Through this work, we fill these gaps in the literature.

2. Methodology Overview

We employ the wearable flexion sensor reported in [2] that consists of electrically small resonant loops wrapped around the limb: one loop is placed above the joint and one loop is placed below the joint. The operating principle of this sensor is analyzed in [2]. In brief, Faraday's law is leveraged to monitor the flexion angle as the two loops misalign, such that changes in transmission coefficient magnitude ($|S_{21}|$) are mapped into flexion angles.

In this work, we first confirm experimentally that textile drift error is indeed an issue and attempt to understand the cause of this error. Next, we report a two-step methodology to correct this error as based upon an initial condition calibration followed by a machine-learning aided calibration. For all cases, our experimental setup is shown in Figure 1. Specifically, a Styrofoam phantom limb is employed with cylindrical shape and ability to flex at the joint [2]. Two loops are wrapped around the limb to serve as the sensor and are connected to a network analyzer for $|S_{21}|$ data collection. Finally, ArUco markers and computer vision are employed for "gold standard" angle collection. A stretchy sleeve serves as the garment on which the sensors are embedded. Selection of stretchy sleeve is based upon our studies reported in [5].

3. Understanding E-Textile Noise

To analyze the pattern of e-textile noise, we used the setup of Figure 1 and studied two configurations: (a) loops without sleeve (control), and (b) loops embedded in stretchy sleeve. We measured $|S_{21}|$ of the loop pair at different flexion angles as well as the "gold standard" angles using a camera and computer vision software.

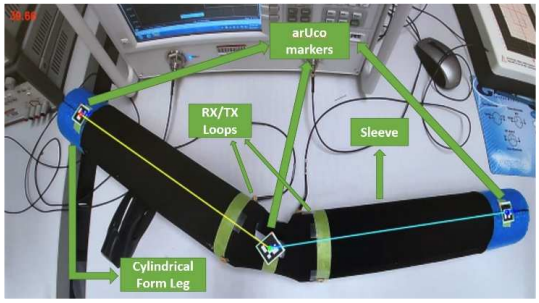

Figure 1. Experimental setup employed in this study.

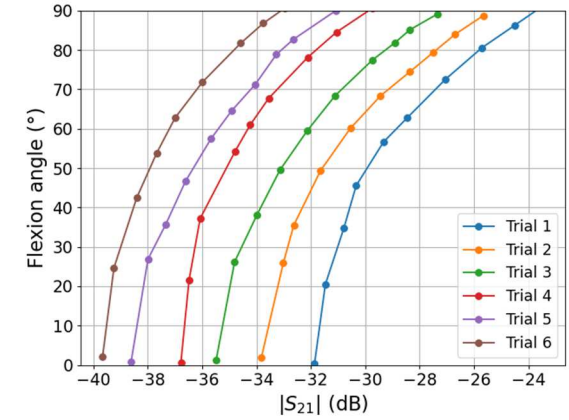

(a)

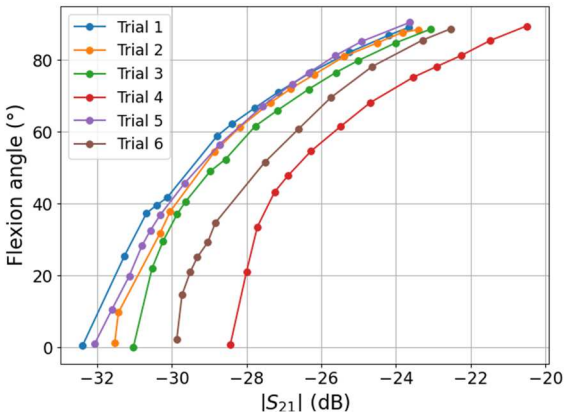

(b)

Figure 2. Flexion angle vs. transmission coefficient: (a) without, and (b) with the sleeve. Trials shown in the legend correspond to different distances between the loops and are not the same between (a) and (b).

Measurements for the two configurations (i.e., without and with the sleeve) are shown in Figure 2. As seen, without the sleeve, $|S_{21}|$ curves are predictable and the curvature pattern remains similar under different conditions (in this case, different distances between the loops represented by different trials). In other words, shifting the curves left and right and taking a weighted average based on their given initial $|S_{21}|$ value (i.e., $|S_{21}|$ value at 0°), one can make a good $|S_{21}|$ curve prediction. This will be critical to the first step of our calibration process discussed in Section 4. By contrast, when the sleeve is integrated, $|S_{21}|$ curves are unpredictable and curvature changes significantly under

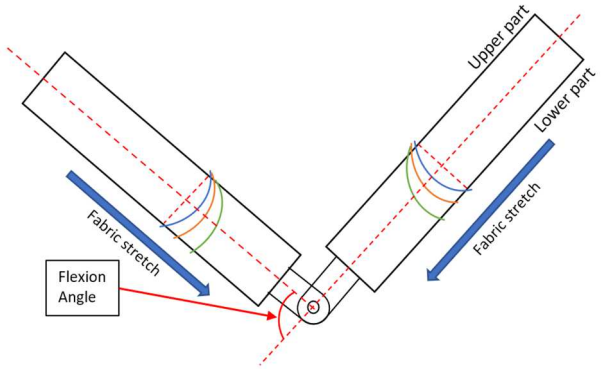

Figure 3. Sleeve stretching model during joint flexion corresponding to Figure 1. Dotted vertical lines represent the ideal location of the loops, while solid lines show the loop displacement under fabric stretch.

different conditions. Note that the Trial 1-6 in Figure 2(a) and Trial 1-6 in Figure 2(b) are not measured under the same corresponding initial condition, i.e., distance between loops. Nevertheless, curves shown in Figure 2(b) still illustrate the issue of drastic change in curvature or curve shape under different initial conditions when sleeve stretching is taken into account.

The difference in shape of the $|S_{21}|$ curves shown in Figure 2(b) can be explained by the model illustrated in Figure 3. When flexion occurs from smaller angles to larger angles, the lower part of the sleeve is stretched more as compared to the upper part of the sleeve. As loops are attached to the sleeve, the lower part of the loop will shift more towards the joint. This causes the relative distance and angle between loops on both sides of the joint to change. Since the $|S_{21}|$ reading relies on the relative distance and angle between the two loops, noise will be introduced with increasing flexion angle, but there will be no noise at 0° flexion angle. Due to this reason, the value of $|S_{21}|$ at 0° remains the same, regardless of whether the individual is wearing a sleeve, as long as the distance between the loops remains the same. This information is crucial for step 2 of the calibration process further elucidated in Section 4.

4. Calibrating E-Textile Noise

The proposed calibration process relies on two steps:

Step 1: Initial condition calibration. By measuring $|S_{21}|$ at a fixed initial position of 0°, the distance between two loops can be identified and, hence, calibrated. In turn, this measurement allows us to determine a model for $|S_{21}|$ vs. flexion angle in the absence of uneven fabric stretching per Figure 2(a). To aid in this calibration, we approximated the curves of Figure 2(a) using regression to get an equation in the form of:

$$\hat{y} = a \cdot log_{10}x + b \cdot x + d. \quad (1)$$

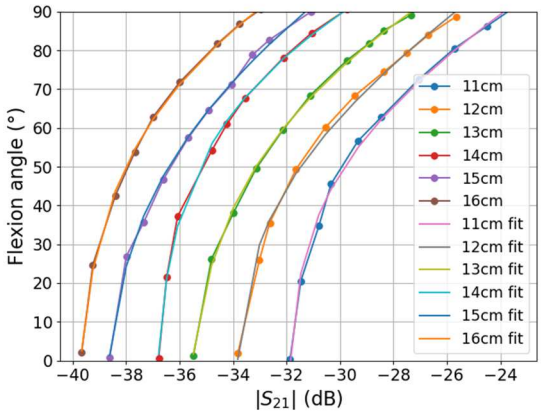

Figure 4. Experimentally collected data and their logarithmic fit curves.

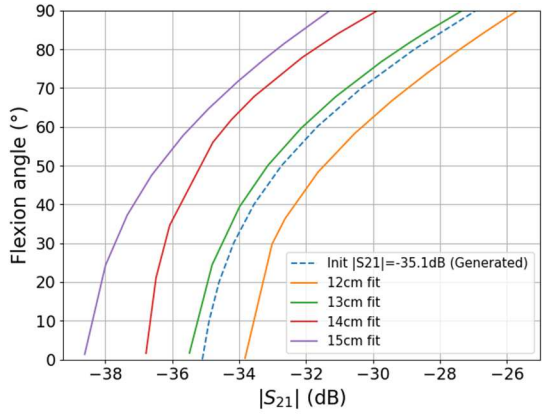

Figure 5. Example of the proposed Step 1 calibration, where a curve is generated for $|S_{21}|$=-35.1 dB at 0° .

Experimentally collected data and their corresponding fitted curves are shown in Figure 4. Other curves lying between these curves can then be readily obtained using equation (1). For example, a curve with $|S_{21}|$=-35.1 dB at 0° would lie between the curves corresponding to a loop distance of 12 cm and 13 cm, respectively. This curve can be generated automatically using this Step 1 calibration, as shown in Figure 5.

Step 2: Machine-learning-aided calibration. Machine learning can then be used as a non-linear regulator to offset uneven fabric stretching noise generated during flexion. Therefore, a calibrated and denoised model of $|S_{21}|$ vs. flexion angle can be calculated for any specific setup.

To achieve the above, a 3-layer neural network is employed, having 48 nodes as hidden layer, as shown in Figure 6. The input of the network is 10 data points for the $|S_{21}|$ curve obtained without considering the sleeve stretches (i.e., $|S_{21}|$ values at 0° , 10° , 20° … 90° from one of the curves of Figure 2(a)). The output of the network is 10 data points for the corresponding $|S_{21}|$ curve that considers the sleeve stretches.

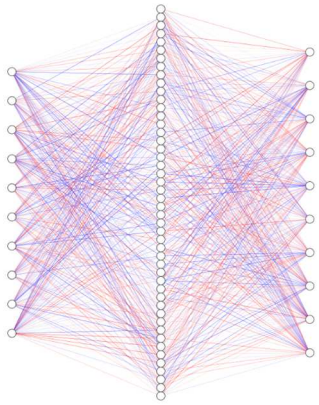

Figure 6. Structure diagram of the neural network employed in this study.

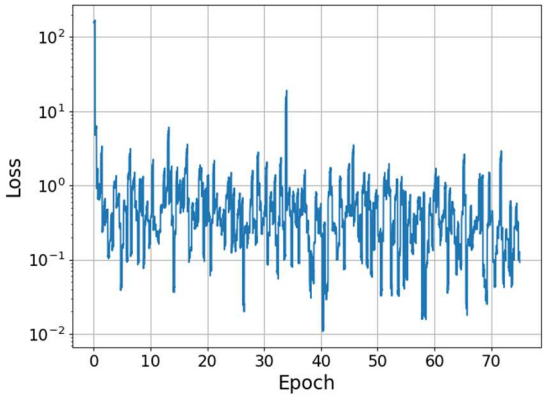

Figure 7. Test loss after 75 epochs of training.

We applied the dropout technique to avoid overfitting problems and, hence, to further improve the test loss [9]. The dropout rate is set to 0.33. We also applied the batch normalization technique after each layer [10] to help re-center and rescale weights in each layer during the back-propagation training phase. This can allow for higher learning rates that boost the training speed.

Overall, 2000 data samples were imported, 1600 of which were used as training samples, and 400 were used as test samples. The batch size was set to 40. After 75 epochs of training, with a learning rate equal to 0.005, and using the Adam Optimization Algorithm [11], we controlled the test loss to a small value, as shown in Figure 7.

An example of the system's performance is summarized in Figure 8. Here, the blue line of the $|S_{21}|$ vs. flexion angle curve without considering sleeve stretches serves as the input of the trained neural network. The output of the neural network is the orange curve, showing the predicted $|S_{21}|$ vs. flexion angle curve that takes sleeve stretches into account. Referring to the dashed green line that represents the experimentally measured $|S_{21}|$ curve for the same initial condition of $|S_{21}|$ = -36 dB at 0° flexion angle, we see excellent agreement. That is, our prediction result is very accurate. The denoised flexion angles can ultimately be obtained via the $|S_{21}|$ readings of this predicted curve. Using this methodology, we demonstrate that the error of the predicted curve can be controlled to under 0.3°.

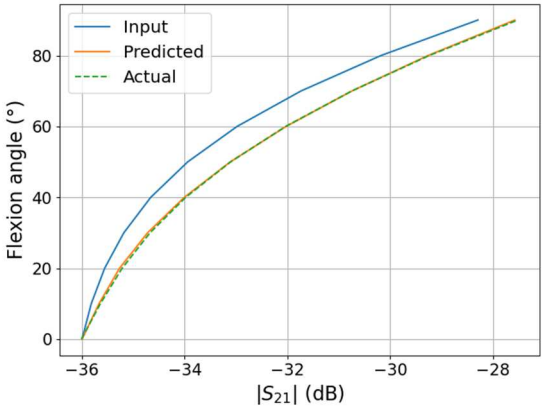

Figure 8. Output generated by trained neural network

5. Conclusion

In conclusion, the error caused by sleeve stretches can be detrimental to the accuracy of joint angle measurements carried out by wearable, textile-based, kinematics sensors. The proposed 2-step methodology can be used to effectively cancel out the error introduced by the sleeve stretches. In the future, we will expand upon this approach for dynamic motion of the human limb and we will validate it on human subjects.

Acknowledgment

This work was supported by the National Science Foundation (NSF) under award 2042644. Yuxuan Han was also supported by a Summer Undergraduate Research Fellowship from The Ohio State University Chronic Brain Injury Discovery Theme. The authors would like to thank undergraduate students Ian Anderson and Chris Cosma for their assistance with the computer vision software.

References

[1] V. Mishra and A. Kiourti, "Wearable Sensors for Motion Capture," in *Antenna and Sensor Technologies in Modern Medical Applications*, John Wiley & Sons, Ltd, 2021, pp. 43–90

[2] V. Mishra and A. Kiourti, "Wrap-around wearable coils for seamless monitoring of joint flexion," *IEEE Transactions on Biomedical Engineering*, vol. 66, no. 10, pp. 2753-2760, Oct. 2019.

[3] V. Mishra and A. Kiourti, "Wearable electrically small loop antennas for monitoring joint flexion and rotation," *IEEE Transactions on Antennas and Propagation*, vol. 68, no. 1, pp. 134-141, Jan. 2020.

[4] V. Mishra and A. Kiourti, "Wearable Radio Frequency Loop Sensors for Monitoring Joint Kinematics," *2021 XXXIVth General Assembly and Scientific Symposium of the International Union of Radio Science (URSI GASS)*, 2021, pp. 1-4.

[5] R. Ketola, V. Mishra, and A. Kiourti, "Modeling fabric movement for future E-Textile sensors," *Sensors*, vol. 20, no. 13, p. 3735, Jul. 2020

[6] Q. Bai and R. Langley, "Crumpling of PIFA textile antenna," *IEEE Transactions on Antennas and Propagation*, vol. 60, no. 1, pp. 63-70, 2012.

[7] B. Hu, G.-P. Gao, L.-L. He, X.-D. Cong, and J.-N. Zhao, "Bending and on-arm effects on a wearable antenna for 2.45 GHz body area network," *IEEE Antennas and Wireless Propagation Letters*, vol. 15, pp. 378-381, 2016.

[8] M. Kok, J.D. Hol, and T.B. Schon, "Using inertial sensors for position and orientation estimation," *Foundations and Trends in Signal Processing*, vol. 11, no. 1-2, pp. 1-153, 2017.

[9] Srivastava, N., Hinton, G., Krizhevsky, A., Sutskever, I. and Salakhutdinov, R., 2014. Dropout: a simple way to prevent neural networks from overfitting. *The Journal of Machine Learning Research*, 15(1), pp.1929-1958.

[10] S. Ioffe, C. Szegedy, "Batch Normalization: Accelerating Deep Network Training by Reducing Internal Covariate Shift," *International Conference on Machine Learning*, 2016 pp. 448-456

[11] D. P. Kingma, J. Ba, "Adam, A method for stochastic optimization," *Computing Research Repository (CORR)*, 2015, 1412, 6980